1475

Design of a shimming coil matched to the human brain anatomy

Feng Jia[1], Hatem Elshatlawy[1], Ali Aghaeifar[2], Sebastian Littin[1], Stefan Kroboth[1], Ying-Hua Chu[1], Yi-Cheng Hsu[1], Xiang Gao[1], Huijun Yu[1], Philipp Amrein[1], Wenchao Yang[1], Jiazheng Zhou[2], Pierre Levan[1], Klaus Scheffler[2,3], and Maxim Zaitsev[1]

[1]Dept. of Radiology · Medical Physics, Medical Center University of Freiburg, Faculty of Medicine, University of Freiburg, Freiburg, Germany, [2]Max Planck Institute for Biological Cybernetics, Tuebingen, Germany, [3]Department of Biomedical Magnetic Resonance, University of Tuebingen, Tuebingen, Germany

Synopsis

We propose a novel design method of a shim coil specially optimized for the human brain. Numerical results demonstrate the validity of the method. The resulting coil layouts can pave a way towards a novel shimming coil specifically intended for human brain shimming. The proposed design method can be extended to other applications and organs.

Introduction

The recent years have seen significant progress in improved shimming for the human brain using higher-order spherical harmonics (SH) coils[1] and multi-coils[2–7]. Although all these coils outperform the routine second order spherical harmonic shimming, coil elements of these coils were not designed with an explicit consideration of the magnetic field maps observed in the target organ. Here we propose a design method for shim coils based on the singular vector decomposition and the stream function method[8] using human-brain field maps. To find an optimal number of coil elements of the array a cross validation technique is applied. The numerical results demonstrate the validity of the design method.

Methods

Whole brain $\mathbf{B}_0$ field maps of twelve subjects in seven head orientations each were acquired. Phase unwrapping and first order shimming (realizable by linear gradients) were applied in post-processing. Each of the resulting field maps was used as a target magnetic field. A stream function on a cylindrical surface of 360 mm diameter and 300 mm length was then optimized to minimize the standard deviation of the residual magnetic field over the whole brain. During the optimization, the coil power dissipation was constrained to obtain a wire pattern of a shim coil with the same residuals as for SH shimming with a certain predefined order (referred to as a target order). Finally, stream functions on the surface were obtained for each of the field maps to form a matrix with 84 columns.

The singular-value decomposition (SVD) was performed on this matrix and the resulting left-singular vectors (referred to as components), corresponding to several largest singular values, were used to obtain wire patterns of coil elements. A performance analysis for a different number of components was then obtained for each brain field map. The standard deviation of the residual magnetic field was minimized and compared to the residual of SH shimming with a given order. The highest SH order inferior to the designed coil is referred to as achieved order while the channel acount corresponds to the minimum number of components to achieve a certain SH shimming capability.

To test the generalization ability of the designed coil, the leave-one-out cross-validation technique[9] was used: out of 12 subjects, eleven subjects were assigned to the training group and one was assigned to the validation group. The procedure was repeated 12 times such that each subject was sequentially assigned to the validation group. Field maps in the training group were used to design a shim coil using SVD, which was then applied to the validation group.

Results and discussions

Figure 1 and 2 show the box plots of the channel counts and maximum dissipated power for the field maps across all validation groups. As seen in Figure 1, the median value of the channel count decreases with the increase of a target order. Moreover, when the target order is equal to, or greater than the achieved order, the median value of the channel count tends to be lower than the total numbers of SH functions. Although the selection of the higher target order can lead to an increase of the maximum dissipated power, as shown in Figure 2, it can be acceptable from an engineering perspective based on previously realized air-cooled coils.

Figure 1b-f show that in some cases the maximum channel count tends to vary in a U-shape with increased target order. In those cases the values at the transition points can be selected as the numbers of coil elements of the designed coil. Examplarily, 12 and 24 can be selected as the total number of coil elements to obtain SH shimming capability of the fourth and fifth order, respectively, for the field maps in the validation groups. Here the target orders are equal to 5 and 6, respectively. Compared with the corresponding SH functions, the total numbers of needed shim channels are reduced to 57 % and 77 %, respectively.

Figure 3 and 4 show scatter plots of standard deviations for all field maps of all subjects using 12 and 24 SVD components compared to higher order SH shimming. Using more than 39 and 90 percent of all the field maps these components lead to equal or better shimming capability of the fifth and sixth order SH shimming, respectively. Figure 5 depicts the first four wire patterns of the 12 components which are very different from conventional SH coil layouts[10].

Acknowledgements

This work was supported by the German Research Foundation (DFG) (Grant Numbers. ZA 422/5-1, ZA 422/6-1 and KS 658/13-1) and the European Research Council Proof-of-Concept Grant ‘mrSANE’ grant agreement 755466.

References

1. Pan et al. Role of very high order and degree B0 shimming for spectroscopic imaging of the human brain at 7 Tesla. Magn Reson Med. 2012;68: 1007-1017.

2. Juchem et al. Magnetic field modeling with a set of individual localized coils. J Magn Reson. 2010;204:281-289.

3. Stockmann et al. A 32-Channel Combined RF and B0 Shim Array for 3T Brain Imaging. Magn Reson Med. 2016;75: 441-451.

4. Han et al. Integrated Parallel Reception, Excitation, and Shimming (iPRES). Magn Reson Med. 2013;70:241-247.

5. Truong et al. Integrated RF/shim coil array for parallel reception and localized B0 shimming in the human brain. NeuroImage. 2014;103:235-240.

6. Jia et al. Using a matrix gradient coil for shimming of the human brain. In: Proc. ESMRMB 2016, s77-s78.

7. Aghaeifar et al. Dynamic B0 shimming of the human brain at 9.4 T with a 16-channel multi-coil shim setup, MRM early view. doi:doi.org/10.1002/mrm.27110.

8. Peeren GN. stream function approach for determining optimal surface currents. J Comput Phys. 2003;191:305-321.

9. Devijver et al. Pattern Recognition: A Statistical Approach. 1982. London, GB: Prentice-Hall.

10. Hudson et al. Finite-length shim coil design using a fourier series minimum inductance and minimum power algorithm, Concepts Magn Reson Part B Magn Reson Eng. 2010;37B:245-253.

Figures

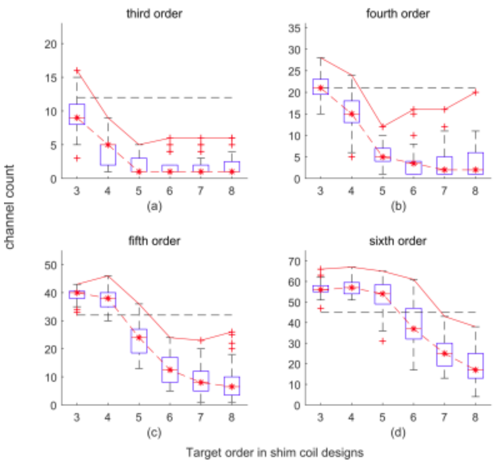

Figure 1. Box plot of channel counts needed to achieve the third-order (a), the fourth-order (b), the fifth-order (c) and the sixth-order (d) SH shimming capability for all the validation data of the residual field maps. To assess the channel counts, the numbers of the corresponding SH components are also displayed as black dashed lines. Here, the numbers of SH components (referred to as SH number) are defined as to be the total number of up to the SH functions for the given order minus four.

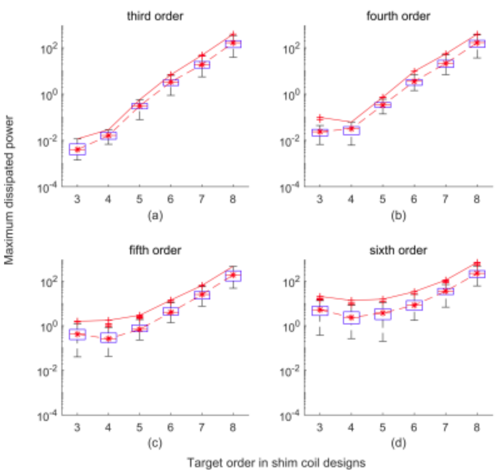

Figure 2. Box plot of maximum dissipated power of the used SVD components needed to achieve the third-order (a), the fourth-order (b), the fifth-order (c) and the sixth-order (d) SH shimming capability for all the validation data of the residual field maps. The variations of the maximum and median values of those maximum dissipated power with respect to target orders are respectively depicted in red solid lines and red dashed lines with the star symbols. The outliers of the maximum dissipated power are plotted using the plus symbols.

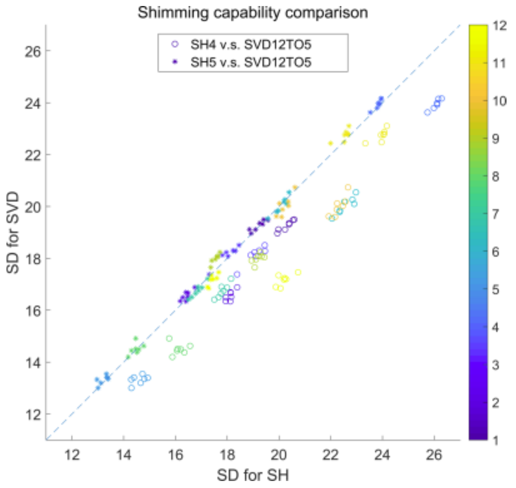

Figure 3. Comparison of standard deviation (SD) between SH shimming and SVD coil shimming for all the data. Here, SH4 and SH5 indicate the fourth and fifth order SH shimming, respectively. SVD12TO5 means that the twelve largest singular vectors are used for shimming when the target order (TO) is 5. Equal standard deviations for two methods are plotted as the dashed diagonal line. SDs for different subjects are marked in different colors.

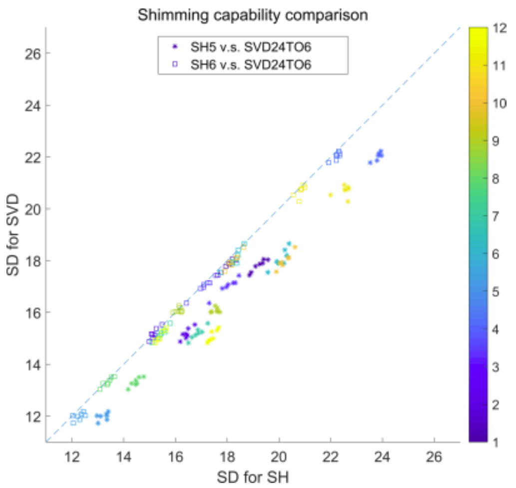

Figure 4. Comparison of standard deviation (SD) between SH shimming and SVD coil shimming for all the data. Here, SH5 and SH6 indicate the fifth and sixth order SH shimming, respectively. SVD24TO6 means that the 24 largest singular vectors are used for shimming when the target order (TO) is 6. Equal standard deviations for two methods are plotted as the dashed diagonal line. SDs for different subjects are marked in different colors.

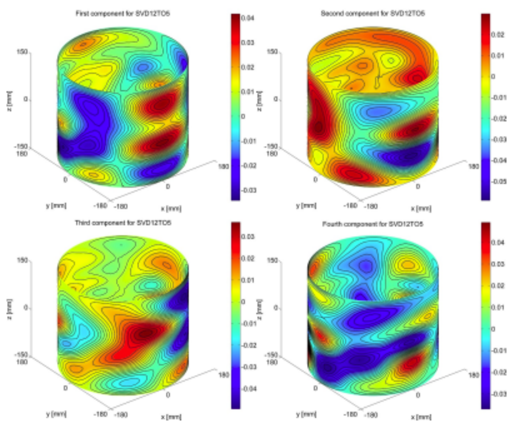

Figure 5. Wire patterns of the first four components in SVD12TO5.